Three-terminal, single molecule circuits based on carbon nanotube interconnects

B.R. Goldsmith[*], J.G. Coroneus[**], V.R. Khalap[*],
A.A. Kane[*], G.A. Weiss[***], and P.G. Collins[*]

Departments of Physics and Astronomy[*], Molecular Biology and Biochemistry[**], and Chemistry[***]
University of California Irvine, Irvine, CA 92697

ABSTRACT

The vision for molecular electronics extends well beyond miniaturization and scaling and includes new techniques for studying chemical reactivity, biocatalysis, and molecular recognition. However, reliable single-molecule devices remain exceedingly difficult to fabricate. We demonstrate a new architecture for studying single-molecule behavior that relies on point functionalization of single-walled carbon nanotube circuits. The technique avoids precision lithography and mechanical manipulation. Instead, nanotube conductance is used to reveal chemical processes happening in real-time and to deterministically control oxidation, reduction, and conjugation to target species. We routinely functionalize pristine, defect-free SWNTs at one, two, or more sites and demonstrate three-terminal devices in which a single biomolecular attachment controls the electronic response. Compared to other fabrication techniques for molecular electronics, this method produces devices with excellent electrical, mechanical, and chemical stabilities and well-defined bonding to the molecule of interest.

Keywords: nanotube, biosensor, functionalization

1 INTRODUCTION AND MOTIVATION

The initial exploration of molecular electronics has focused on two main architectures [1]. In the first architecture, molecules bridge the gap between two electrodes which have been tailored to have the smallest possible size. In the second, two crossing nanowires define a zero-dimensional intersection in which a molecule can sit.

Figure 1 depicts these two architectures as well as a third in which a molecule is bound to the sidewall of a single-walled carbon nanotube (SWCNT). In principle, this third design takes advantage of the size of a SWCNT to provide the smallest possible electrical contacts to a single molecule or cluster [2, 3]. Because of the SWCNT's small profile and extreme aspect ratio, these contacts simultaneously provide excellent experimental access to the molecule in question – whether by electric and electromagnetic fields, which are typically shielded by larger electrodes, by electrolytes or binding agents that give the molecule its chemical functionality, or by other local probes including microscopy.

In the implementation described below, a point defect in a SWCNT is used as a versatile attachment site for different moieties. Nearly the entire resistance of the SWCNT device is localized at such a defect, providing a high degree of sensitivity to any attachment of interest. Despite some advantages, this SWCNT architecture is functionally more complex and, in particular, does not directly measure a molecule's conductance. Instead of attempting to pass an electrical current directly through a molecule (and its linkages), the design moves charge through an insulating region closely coupled to the molecule of interest. While less direct than the more conventional architectures, these versatile SWCNT devices can link a wide range of molecules and potentially incorporate all of the functionality motivating the molecular electronics field more generally.

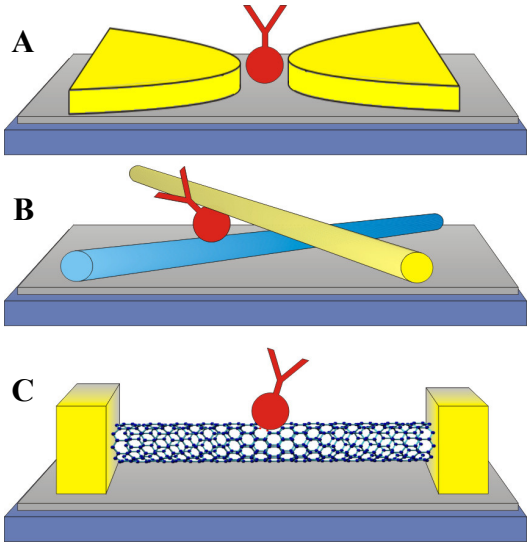

Fig. 1: Three example architectures of molecular devices. In the SWCNT case, one or more lattice defects simultaneously serve as the attachment site and as an electrically-insulating break (**C**).

2 EXPERIMENTAL METHODS

Field-effect transistor devices with single-SWCNTs as the conducting channel were fabricated using standard techniques. Briefly, SWCNTs were grown by chemical vapor deposition on a thermally oxidized silicon substrate and then contacted by metal electrodes (Ti or Pd) defined by optical lithography. Often, multiple independent devices

were fabricated from the same SWCNT, each having a channel length of approximately 2 μm.

The devices were modified in a custom electrochemical cell in which the SWCNT circuit was configured as a working electrode [4]. Platinum wires were used as counter and reference electrodes, and the electrochemical deposition potentials were controlled by a customized potentiostat system. While monitoring the SWCNT conductance *G*, the potential of the cell was raised to match or exceed the oxidation threshold of the SWCNT.

Electrochemical oxidation readily attaches adducts to a SWCNT sidewall [3, 5], and these groups can serve as sites for further chemical derivatization. For example, metal species preferentially deposit on oxygen-containing defects such as epoxides and can be used to decorate point defects [6]. The chemistry of the defects can be tailored using, for example, electrochemical reduction to produce ethers or further oxidation in $KMnO_4$ to produce carboxyl groups. Finally, bioconjugation to these sites can be performed using *N-ethyl-N'*-(3-dimethylaminopropyl) carbodiimide (EDC) and *N*-hydroxysuccinimide (NHS) [7].

To produce devices with single molecule sidewall attachments, it is necessary to limit the initial oxidation to a single adduct. Fortunately, the one-dimensionality of conduction in SWCNTs makes the two-terminal device conductance exquisitely sensitive to single point defects. As described below, the dynamics of G(t) during oxidation clearly resolve the creation of individual sites. For this conductance-monitoring technique to be successful, connective metals and other sensitive interfaces must either be inert or be protected from chemical attack. Coating the devices with polymethyl methacrylate (PMMA) protected the majority of the device while allowing small portions of the SWCNT sidewall to be exposed by electron beam lithography.

3 RESULTS AND DISCUSSION

Fig. 2 depicts the typical changes in conductance observed when electrochemical oxidation is initiated on a SWCNT device. As adducts covalently add to the SWCNT sidewall, sharp drops and multi-level metastability are observed in *G(t)*. The transition width of each step is usually faster than our experimental resolution of 10 μs, but the timing between steps is stochastically distributed on a scale of seconds. Slowing the reaction by biasing near the oxidation threshold help to clearly resolve individual events, even when the full 2 μm channel of SWCNT is exposed.

Characterization of the oxidized devices indicates that the change in *G* is localized to a small region of the SWCNT. Scanning probe techniques such as scanning gate microscopy (SGM), Kelvin probe force microscopy (KFM), and electrostatic force microscopy (EFM)[8] have all been used to directly image the local transconductance and potential gradients and of the oxidized sites [3]. Selective electrodeposition [6] similarly labels individual sites on the

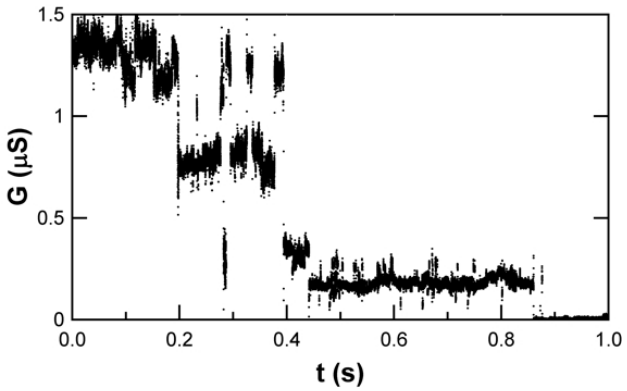

Fig. 2: Real-time electrochemical oxidation of a SWCNT sidewall, measured at +0.6 V vs. Pt in 15 M HNO_3.

oxidized SWCNTs. The resistance mapping is complementary to the chemical labeling and proves the one-to-one correspondence between local resistance and chemical reactivity.

Following oxidation and local mapping, additional chemistry can be used to tailor the oxidized sites. In particular, EDC/NHS is a chemoselective route for conjugating carboxy-terminated SWCNTs to amines [9]. An efficient EDC/NHS protocol, which includes a brief pretreatment with $KMnO_4$ to fully oxidize any attachment sites, has led to reliable point attachment of multiple types of proteins [3]. An example using Au-labeled streptavidin is shown below in Fig. 3.

The locally-oxidized SWCNT region is advantageous for multiple reasons. First and foremost, it restricts successful bioconjugation to a single site on the device. This self-limiting constraint allows long incubation times and high protein concentrations to be used to improve the

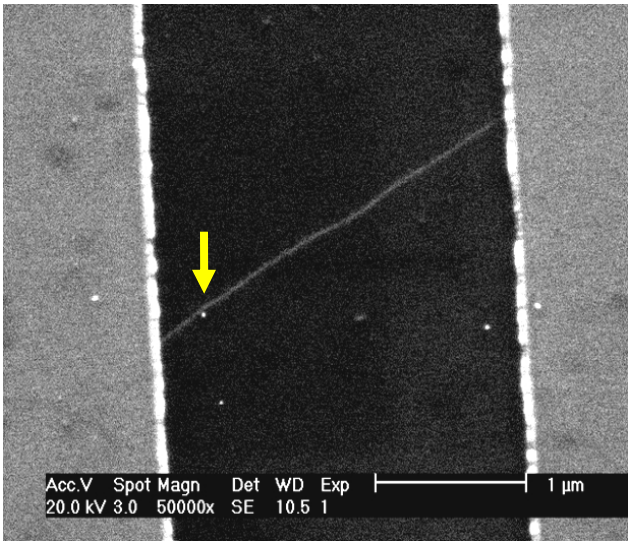

Fig. 3: SWCNT device to which one molecule of streptavidin has been covalently attached (arrow). The protein itself is not visible but has been labeled with a 20 nm Au particle for imaging.

attachment yield at the SWCNT's selected site without causing gross, nonspecific surface contamination. Second, the electronic properties of the oxidized region concentrate the device's resistance at the exact spot of chemical attachment. The device constitutes a one-dimensional, metal-insulator-metal heterostructure in which only the insulating region displays the correct surface chemistry for attachments. Finally, the oxidized region provides a stability to the device which is not present when etching or ablation is used to mechanically split a SWCNT [2]. Oxidized devices have been thermally cycled from 4 – 600 K with no sign of mechanical degradation [3, 4], though of course biomolecular attachments do not survive such treatment.

Once constructed, these circuits exhibit interesting dynamic noise and fluctuations, which are presumably due to their molecular attachments.

A simple example is shown in Fig. 4. A $KMnO_4$-treated SWCNT containing one or more carboxy-terminated groups exhibits small current fluctuations whether measured in air or aqueous buffer [10] (Fig. 4A). These fluctuations have a 1/f spectrum typical for SWCNT conductors [11]. A more complex, two-level fluctuation is sustained when 10 μM EDC is added to the buffer (Fig. 4B). Since carboxyls strongly influence *G* and are known to be briefly modified by EDC, the additional switching may be attributed to this chemical process. The high current level, which has a mean lifetime of 1 – 10 ms, provides direct insight into the kinetics of the EDC activation, potentially with single molecule resolution.

More complex measurements are possible using biofunctional devices. For example, the protein lysozyme has been attached to point-oxidized SWCNTs using the same EDC/NHS protocol described above. Lysozyme-functionalized SWNTs exhibit a dynamic conductance noise which depends on whether the appropriate biological substrate is present in the surrounding buffer. While the 1/f spectrum is uniform and featureless in buffer, the addition of substrate produces a new spectral peak which meanders between 400 and 500 Hz over the hour-long duration of the experiment. An effective way to represent this effect is to plot the spectrum of conductance fluctuations versus time as shown in Fig. 5. In this greyscale plot, the substrate-dependent peak is clearly distinguishable from the background 1/f noise and 60 Hz harmonics. Identification of such peaks is possible even when the fluctuator is too weak to be directly observed in real-time data like Fig. 4.

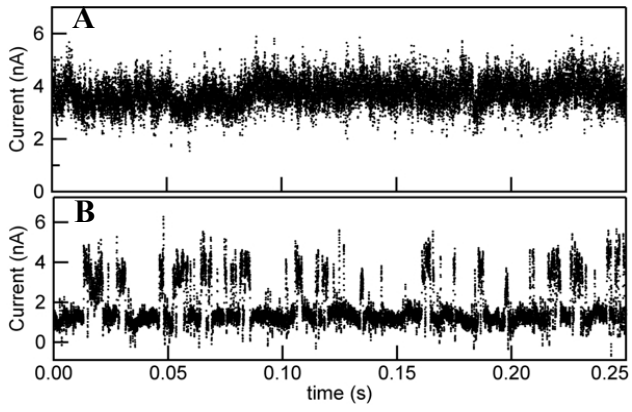

Fig. 4: Current vs. time for a point-oxidized SWCNT device with carboxyl terminations, in buffer (A) and in buffer with 10 μM EDC.

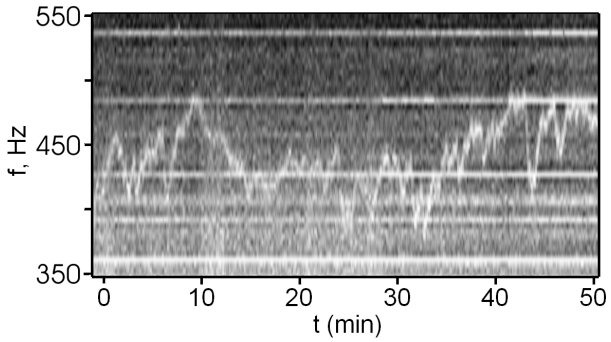

Fig. 5: Conductance power spectrum, in greyscale, versus time for a lysozyme-functionalized SWCNT device. Flat horizontal lines are due to device- and time-independent instrumental noise.

4 SUMMARY

The attachment of single species to electronic SWCNT devices provides a versatile platform for studying a wide range of molecular processes. The device conductivity is highly dependent on the attachment site, and it thereby provides a wide bandwidth, *in situ* transducer of chemical activity. While single-molecule readout is clearly demonstrated, additional work will be necessary to determine the full range and applicability of this sensitivity.

This work has been supported by the NSF #EF-0404057 and #DMR-023-9842 (PGC), and the NIH National Institute of General Medical Sciences R01-GM078528-01 and NIAID R43-AI58365-01 (GAW).

REFERENCES

[1] McCreery, R.L., *Chemistry of Materials* **16** (23), 4477-4496 (2004).
[2] Guo, X., et al., *Science* **311**, 356-9 (2006).
[3] Goldsmith, B.R., et al., *Science* **315**, 77-81 (2007).
[4] Mannik, J., et al., *Phys. Rev. Lett.* **97**, 16601 (2006).
[5] Sumanasekera, G., J. Allen, and P. Eklund, *Mol. Cryst. Liquid Cryst.* **340**, 535-540 (2000).
[6] Fan, Y., B.R. Goldsmith, and P.G. Collins, *Nature Materials* **4** (12), 906-911 (2005).
[7] Staros, J.V., R.W. Wright, and D.M. Swingle, *Analytical Biochemistry* **156** (1), 220-222 (1986).
[8] Bachtold, A., et al., *Phys. Rev. Lett.* **84** (26), 6082-6085 (2000).
[9] Wong, S.S., et al., *Nature* **394** (6688), 52-55 (1998).
[10] Phosphate buffer consists of 0.02 M dibasic sodium phosphate buffered with phosphoric acid to pH 4.5.
[11] Collins, P.G., M.S. Fuhrer, and A. Zettl, *Appl. Phys. Lett.* **76** (7), 894-896 (2000).